


Article

# Fire Scars Negatively Affect Hydraulic Conductivity in White Oak (*Quercus alba*)

Justin R. Dee <sup>1,\*</sup>, Michael C. Stambaugh <sup>1</sup>, Kevin T. Smith <sup>2</sup>  and Daniel C. Dey <sup>3</sup>

<sup>1</sup> Missouri Tree-Ring Laboratory, School of Natural Resources, University of Missouri, 203 ABNR Building, Columbia, MO 65211, USA; stambaughm@missouri.edu

<sup>2</sup> U.S. Forest Service, Northern Research Station, 271 Mast Road, Durham, NH 08324, USA; ktsmith@fs.fed.us

<sup>3</sup> U.S. Forest Service, Northern Research Station, 202 ABNR Building, University of Missouri, Columbia, MO 65211, USA; daniel.c.dey@usda.gov

\* Correspondence: deejr@missouri.edu

Received: 8 July 2019; Accepted: 9 September 2019; Published: 18 September 2019



**Abstract:** Fire management is increasingly used to manage forest stand structure and dynamics. Relatively intense fires can injure the tree stem and induce fire scar formation, affecting subsequent tree growth and wood quality. Here, we consider the physiological effects of fire scarring in white oak. Potential hydraulic conductivity, estimated from the mean vessel area and vessel number, was determined for growth rings formed before, during, and after the year of injury. We measured vessel anatomy using the ROXAS image analysis tool on the cross-sections of 14 white oaks of various ages with fire scars originating in different years through the late 19th and early 20th century. We found that the mean vessel area and potential hydraulic conductivity were significantly reduced for the year of and the year immediately following fire injury. After this two-year period, mean vessel area returned to levels present in wood formed prior to the injury. Age when scarred, radius from the pith when scarred, scar height above ground, and percentage of circumference scarred did not explain the degree to which potential hydraulic conductivity was lost in the fire scar year compared to the year prior. Overall, the magnitude of reduction in potential hydraulic conductivity was small but significant. An earlier study on the same cross-sections verified no reductions in radial growth after fire injury. Thus, it is likely that the conductance of older rings is adequate to sustain conductance. Nonetheless, we recommend further investigation, in particular, the ability to predict how tree size, age, position along a slope, and other variables may influence the degree of wounding and possible losses of potential hydraulic conductivity after the fire. Information like this for white oak and other common tree species may help elucidate the physiological impacts fire injuries have on trees existing in forest stands with periodic fire.

**Keywords:** potential hydraulic conductivity; ROXAS; mean vessel area; dendrochronology; fire ecology; fire scars; detrending time-series

## 1. Introduction

One of the most well-known themes in forest ecology is the connection between fire and the global occurrence of oak-dominated forests. For millennia, oak has dominated a variety of landscapes that experience recurring and frequent fire [1–4]. From adaptations in mature trees related to minimizing injury and mortality [5,6], through the regeneration of new cohorts that persist through repeated fires by sprouting to gain a competitive advantage in post-disturbance environments [7–9], fire can play a central role in maintaining the structure and composition of oak-dominated forests [7,10,11]. In the U.S., the dendroecology of the Midwestern forests reveals complex relationships among forest composition and structure, climate, and fire from both natural and anthropogenic causes [12–17].

Despite the evidence of enhanced oak regeneration and productivity after fire [18], the response of forestry professionals to prescribed burning is mixed, as fire can kill and damage individual trees and contribute to a considerable economic loss [19]. Indeed, fire can cause top-kill, interrupt wood formation for a portion of the stem circumference, reduce overall growth increment, and provide entry for wood decay fungi which could reduce merchantable volume and value [5,20]. Several studies in the Central Hardwoods Region (with focus on the Ozark Highlands) found little reduction in log grades and volume of decayed wood in oak species several years after fire exposure [21–24]. Important determinants of tree mortality and extent of economic value loss include the degree of fire injury as indicated by observations on fire scars and tree-related factors, including age and diameter when scarred [21–23].

Fire injury that results in fire scars occurs by convective and radiative heat transfer through the bark, killing the vascular cambium, and subtending sapwood [25]. In response, the tree forms compartmentalization boundaries and barriers to resist the loss of sapwood function and the spread of infection by wood decay fungi and other microorganisms [26]. Wood production is stimulated at the wound margin, producing ribs of woundwood that tend to close over the wound. Woundwood contains a higher percentage of enlarged and suberized parenchyma and shorter conducting elements than normal wood [27]. The anomalous anatomy diminishes with increasing tangential distance from the wound margin. For open fire scars, the woundwood ribs frame the exposed face of the wound, contributing to the “catface” appearance. Depending on the size of the wound, and tree vigor and vitality, the wound may close, thus restoring circumferential continuity of the vascular cambium as has been described for white oak (*Quercus alba*) in northern Missouri [6].

Previous research on the effects of fire injury on wood production has focused on annual ring width and wood volume. Changes in anatomy and physiology in wood formed after injury beyond the hyperplastic woundwood have not been reported, although such changes could affect tree resilience to drought and other stressors. Hydraulic conductivity, the degree to which water can be moved through xylem, is critical to overall tree function [28]. Unlike many ring-porous and all diffuse-porous hardwood species, hydraulic flow in the stem of white oak occurs in the outermost ring or two of sapwood [29]. Fire injury results in embolism formation and blockage of hydraulic flow in the immediate vicinity of the scar [30]. The precise mechanism of injury could either be a non-specific response to mechanical injury akin to partial girdling [25] or from the specific effects heating [31]. In either case, fire injury would aggravate the effects of moisture stress and increase the vulnerability of the tree to hydraulic failure of the stem as a whole.

The objective of this research was to determine changes in potential hydraulic conductivity for individual rings associated with fire scars, extending the investigation on the growth and physiology of white oak [6]. For rings formed prior to and following fire injuries, we estimated potential hydraulic conductivity from anatomical measurements. We considered how scar height, tree age when scarred, tree diameter when scarred, and percent of the circumference scarred affected the relationship between potential hydraulic conductivity and fire injury. Given this is the first study of its kind to our knowledge, we also considered several methodological approaches to detrend and standardize these time series to reduce the confounding effects of tree age and climate [32–35].

## 2. Materials and Methods

The study site was located at Rudolf Bennitt Conservation Area (RBCA, 39.25.12° N, –92.43° W) 35 km north of Columbia, MO, USA. The climate is humid-continental with a mean total annual precipitation and temperature of 109.2 cm and 12.5 °C, respectively [36]. The terrain consists of gentle to rolling hills with slopes ranging from 0 to 15 degrees. Soils are well-drained clay loams that are glacial till in origin. The main forest type of the site is oak-hickory with dominant tree ages ranging from 80 to 150 years. The forest is dominated by white oak, and the major associations are black oak (*Q. velutina*) and post oak (*Q. stellata*). RBCA has a history of grazing, logging, and burning in the last century. Since 2001, the Missouri Department of Conservation has managed about 240 ha of the oak

woodland at RBCA with a mixture of timber stand improvement, commercial harvests, and prescribed fire management.

In the early spring of 2015, 43 recently cut or naturally dead fire-scarred white oaks ranging from 9.1 to 52.1 cm in diameter measured 1.4 m above groundline were sampled within the RBCA woodland management area for the original fire scar closure rate study [6]. The resulting cross-sections from these trees were also used for the present study. The 43 sampled trees had embedded fire scars (wounds that successfully closed within several years after occurrence). Given the original goal of documenting fire scar closure rates among the different tree and climate-related variables, the 43 trees represented a wide range of tree sizes (dbh), scar sizes, and scar ages. For each sampled tree, site conditions noted were: slope, aspect, slope position, canopy position, the basal area surrounding the tree, and percent ground cover under the canopy. One to three cross-sections were obtained from the 43 trees by first felling the trees and obtaining a cross-section near the ground level (Figure 1). Ground-level cross-sections were immediately analyzed for locations of fire scars about the cross-section. A primary fire scar was chosen based on having a viewable period of scar closure (i.e., little to no wood decay prior to the fire scar year and for all post-fire growth rings) that was unaffected by subsequent scarring. The height of this primary scar was determined by cutting up the bole. A second cross-section for each tree was obtained at the top of this scar. In some cases, a third cross-section at the height of the midpoint of a scar was obtained from a tree if the height of the scar was >50 cm in height from the ground.

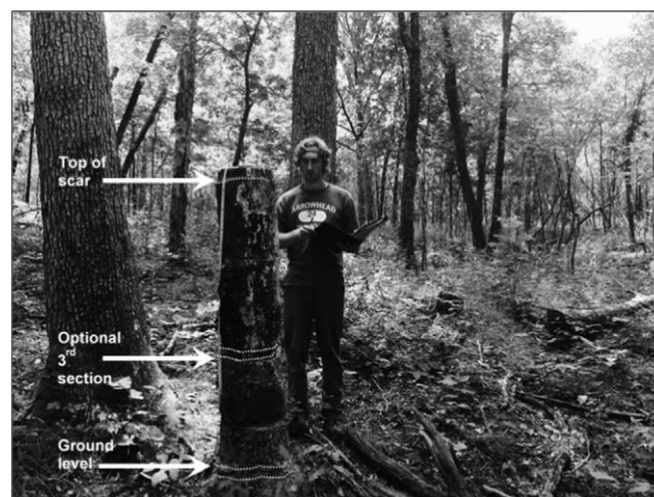


**Figure 1.** Field conditions at Rudolf Bennitt Conservation Area near Columbia, Missouri. Arrows indicate the height at which the cross-sections were collected along the tree bole.

A total of 61 stem cross-sections were obtained from the 43 trees. In the laboratory, one transverse surface of each cross-section was planned and sanded to reveal the cellular detail of wood anatomy corresponding to growth rings and fire scars. Radial tree-ring width was measured (0.01 mm precision) with a Velmex measuring system (Velmex, Inc., Bloomfield, NY, USA) and ring-width series were crossdated using standard dendrochronological techniques [37] and checked with COFECHA software version 6.06p [38,39]. This supplied calendar years for fire scars, pith, and outermost years of growth.

In the fall of 2018, we prepared the same 61 cross-sections for analysis of the vessels in rings formed five years before to five years after a cambial response to injury from a dormant season fire (11 years in total). First, we used a pressure washer set to approximately 1500 pounds per square inch to blast tyloses out of vessels in each cross-section. After air-drying, we discarded the cross-sections which had any substantial amounts of previous decay or wood chipping (possibly from the power washing of decayed wood) in areas of the circumference corresponding to the 11 years under analysis. For cross-sections that had minimal amounts of decay or chipping, we used a black permanent marker to color the wood and then applied talc powder to fill in the vessels. After brushing and blowing away

excess powder, the whole process provided maximum black-white contrast between the vessels and the surrounding wood for subsequent image analysis (Figure 2).

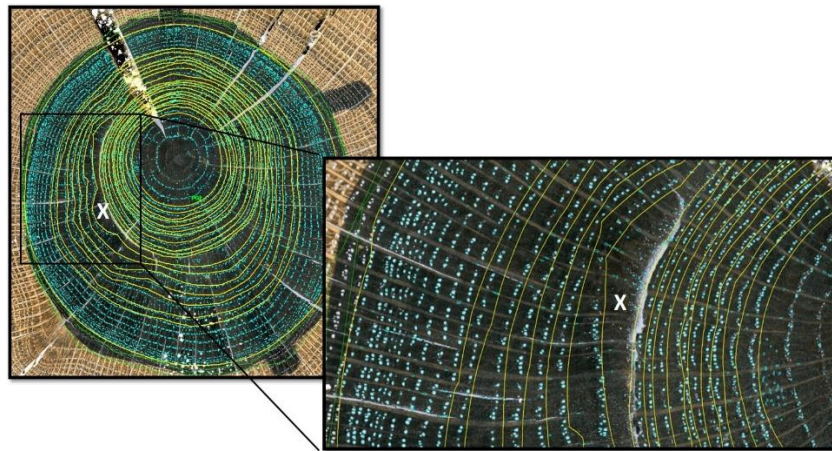


**Figure 2.** Cross-sectional image of white oak growth rings analyzed with the image analysis software ROXAS. To aid visualization, the areas of interest in the white oak cross-sections were blackened and then talc powder was applied to provide contrast for the vessels. After calibration, ROXAS automatically detected vessels (highlighted with a cyan color). The number of vessels, mean vessel area, and potential hydraulic conductivity ( $K_r$ ) were calculated for each growth ring. Yellow lines were manually placed by the researcher to distinguish between rings (not exact ring boundary). X marks the ring associated with a fire scar for this image.

Out of the 61 cross-sections described above, only 20 were found to have satisfactory wood quality to undergo analysis for the present work. An additional six cross-sections were eliminated as the series were too short for climate detrending (explained below). Thus, all analyses below are based on the final 14 cross-sections. Most of the 41 cross-sections not adequate for analyses had a degree of decay that affected parts of the circumference of the 11 years of interest. A small percentage of these had decay specifically in the years that preceded the fire scar, that may still have been adequate for ring measurements, but with a quality of the wood (e.g., lack of decay, anatomical detail) that was decreased beyond the accuracy needed for this study. The decay causes imperfections on the surface of the wood and cracking of vessels which would compromise the accuracy of vessel detection in image analysis software and measurements given the preparation and contrast needed to enhance vessel detection. Additionally, twelve of the 43 cross-sections were not usable due to wood surface chipping caused by power washing partially decayed wood. Wood chipping leads to the same vessel detection discrepancies with image analysis software as decay.

For the 14 cross-sections used in this study, surfaces were scanned at 2400 dpi using an Epson Regent Instruments LA2400 area-calibrated scanner with images acquired by the Epson SilverFast Ai IT8 v8 software. The image files of the whole circumference of the cross-sections (jpeg format, Figure 2) were imported into ROXAS [40]. ROXAS is an image analysis program for quantifying wood anatomical traits. The calibration of ROXAS settings to recognize earlywood vessels amongst all other cell types was necessary for accurate vessel detection and measurements. After several rounds of tests, we found that a threshold cell size between 34,000 to 400,000  $\mu\text{m}^2$  with a roundness factor threshold between 2.25 and 2.6 captured >90% of the earlywood vessels from each ring; latewood vessels (which are usually <30,000  $\mu\text{m}^2$  in size) were not counted in the analysis (Figure 2). Each image was run through the ROXAS process of image sharpening and other contrasting techniques before proceeding to the automatic detection of the vessels in each ring. After rings were manually assigned calendar years, the 11 rings of interest (including the fire scar year) were manually inspected to delete misidentified vessels and to add vessels which were missed by automatic detection. When needed, correction of the vessel shapes and areas was done using the cell editing toolbox in ROXAS.

We obtained the following three values for each of the 11 annual rings under consideration: 1. The total number of vessels, 2. The mean vessel area (MVA), and 3. The potential tree-ring specific hydraulic conductivity (Kr). The vessel area is measured as the white lumen space of each vessel. The Kr for each ring is the sum of Kh (hydraulic potential conductivity) calculated for each vessel contained within the ring based on Poiseuille's law adjusted for elliptical tubes [41], according to the Formula (1):

$$K_h = \frac{\rho \cdot CA \cdot m}{\eta \cdot k} \quad (1)$$

where  $\rho$  is the density of water, CA is the area of the lumen of the respective vessel, m is the mean hydraulic radius calculated for elliptical section tubes,  $\eta$  is viscosity of water, and k is a coefficient depending on the eccentricity of the ellipse. Thus, Kr for each ring is a direct function of both the number of vessels contained within the ring, as well as the MVA. The units for Kr are in terms of  $\text{kg m MPa}^{-1} \text{ s}^{-1}$ .

To assess the impact that fire scarring may have on potential hydraulic conductivity, we first developed an 11-year time series for each sampled cross-section. This 11-year time series consisted of information from rings five years pre-scar (lag-5 to lag-1), the year of the fire-induced cambial injury resulting in the fire scar (lag0), and the five rings post-scar (lag1 to lag5). The time series included the raw values for vessel number, MVA, and Kr for each ring. Given that each successive tree ring is formed to the outside of the stem cylinder, ring circumference increases each year. If ring width, vessel area, and vessel frequency remain stable, the total vessel number and vessel area increase each successive year. Our analysis found an approximately exponential increase in MVA and Kr with an increasing age of the tree at the time of ring formation. The vessel number had a better linear fit with age, though the linear correlation coefficient for vessel number was only 0.02 greater compared to an exponential fit. Thus, for consistency, we removed age-related effects on Kr, MVA, and vessel number by fitting an exponential curve to each tree (Supplementary Figure S1). Using the raw data from each time-series, age detrending was done in R Studio 1.1.453 [42,43] by dividing the raw values by a best-fit positive exponential function; the same way tree-rings are detrended for age [44].

The last step before analyses was to detrend vessel number, MVA, and Kr by the most highly correlated monthly climatic variable so any relation with a cambial response to fire may be amplified. For this effort, the vessel number and MVA were measured, and Kr estimated along 2–4 transects across the entire cross-section from the bark to the pith. These transect measurements were averaged by cross-section, detrended for tree age, and used to build a site chronology of each variable. Those vessel chronologies were correlated to the monthly sum of the precipitation (ppt), monthly average daily maximum temperature (tmax), and monthly average daily maximum vapor pressure deficit (VpdMax) for the years 1895–1969. All climatic data were obtained from the parameter-elevation regressions on independent slopes model PRISM Climate Group [36] (PRISM. Available online: <http://prism.oregonstate.edu/explorer/>, (accessed on January 12th 2019)). For these vessel-climate correlation analyses, we used a 21-month climate window from January of the prior year through to September of the current year. Correlative climate analyses were done using R Studio 1.1.453 [42,43]. We separately chose the highest correlated monthly climatic variable for Kr, MVA, and vessel number and divided their climate functions (the predicted values of Kr, MVA, or vessel number based on regressions with the highest correlated monthly climatic variable) under the already age-detrended values. This final step produced an 11-year age and climate-detrended time-series for each cross-section that was used for further analyses.

Estimated as the product of the two-tailed t-statistic for 10 degrees of freedom and the standard error of the mean, we determined the 95% confidence intervals for raw, age-detrended, and climate-detrended time-series for the 11-year period associated with primary fire scars. For each time course, we also used one-way ANOVA with Tukey posthoc comparisons to find significant differences of vessel number, MVA, and Kr between the scar year (lag0) and all other years (e.g., lag-5 to lag5). To address our main objectives regarding the effect of tree-related variables on estimated hydraulic conductance (Kr),

we used the age- and climate-detrended 11-year time series for each cross-section and calculated the percent change in vessel number, MVA, and Kr between the fire scar year and the preceding year. We determined the Pearson correlation coefficients of the percent change of vessel number, MVA, or Kr to tree characteristics. For series with more than two significant relationships between a percent change and tree-related variables, we ran backward stepwise regressions to identify the tree characteristics with the strongest relationship to Kr. All statistical relationships described in this portion of our analyses were determined by the SPSS software version 25.0 (Chicago, IL, USA).

### 3. Results

#### Significant Effects of Fire on Detrended Kr Time Series

For the final 14 cross-sections used in all subsequent analyses, Figure 3 shows the 95% confidence interval for mean vessel number, MVA, and Kr for raw, age-detrended, and age- and climate-detrended time series over the 11-year time course, respectively. The variation in the raw data yielded wide confidence intervals with no significant differences among the means (Figure 3a). Raw data show an exponential increase for each of the anatomical variables, particularly in the number of vessels (Figure 3a).

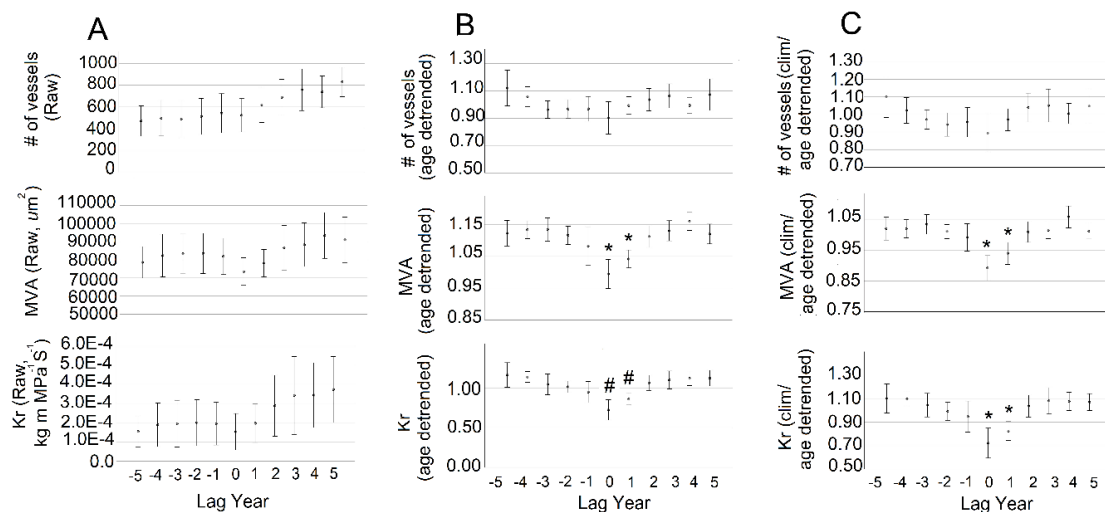


**Figure 3.** 95% confidence intervals for time-series of the 14 cross-sections showing the average of number of vessels, mean vessel area (MVA), and potential hydraulic conductivity (Kr), respectively for each year under the 11-year time-series which includes the fire scar year (lag0) at the center. **(A)** 95% confidence intervals for raw time-series: No significant differences were found in any time course according to one-way ANOVA. **(B)** 95% confidence intervals for age-detrended time-series: For MVA and Kr, the scar year and one-year post-fire had significantly decreased values ( $p < 0.001$ , signified by “\*”) compared to all other years according to one-way ANOVA and Tukey posthoc comparisons, Kr for lag0 and lag1 were marginal decreases ( $p = 0.071, 0.086$ , respectively, signified by “#”). No significant differences were found for the number of vessels between the years of analysis. **(C)** 95% confidence intervals for the age- and climate-detrended time-series: For MVA and Kr, lag0 and lag1 had significantly decreased values ( $p < 0.001$ ) compared to all other years according to one-way ANOVAs and Tukey posthoc comparisons. No significant differences were found for the number of vessels between the years of analysis.

Detrending the series by age reduced variability within the mean values. The lag0 and lag1 rings significantly decreased in MVA and Kr (Figure 3b) as determined by ANOVA and mean comparison. For MVA, lag0 was significantly less than all other years except lag1 ( $p < 0.010$  for all significant comparisons, Figure 3b). Kr was similar, with lag0 being significantly less than all other years, except lag1; however, the difference was only marginally significant with lag−1 ( $p < 0.071$ , Figure 3b). With age

detrending, the vessel number was still not significantly different amongst years. Lag1 was not significantly different from lag0 for MVA or Kr.

Climate detrending had relatively less impact on the identification of fire effects than age detrending (Figure 3c). Climate detrending also reduced the final sample size from 20 to 14 cross-sections; otherwise, satisfactory cross-sections contained series that preceded the availability of the PRISM climate data. A second limitation for the final 14 cross-sections, was the low sample depth for earlier-formed rings. Consequently, we restricted testing the climate relationships to the 1920–1940 period for which 75% of the 14 cross-sections were represented. For this period, the monthly climate variable that was used to detrend the Kr time-series was the June totala monthly precipitation (ppt). We found a highly positive correlation between the current year June ppt and Kr ( $r = 0.601$ ,  $p < 0.001$ , Figure 4) along with a nearly identical inverse relationship with June tmax ( $r = 0.563$ ,  $p < 0.001$ , Figure 4). Also, we noted strong correlations with the previous December tmax ( $r = -0.455$ ,  $p < 0.001$ , Supplementary Figure S2), ppt ( $r = 0.446$ ,  $p < 0.001$ , Supplementary Figure S2), and average maximum daily vapor pressure deficit VpdMax ( $r = -0.377$ ,  $p < 0.001$ , Supplementary Figure S2). MVA was most highly correlated with April tmax ( $r = -0.503$ ,  $p < 0.001$ , Supplementary Figure S2). April of the prior year and November ppt were also highly correlated with MVA (Supplementary Figure S2). MVA was climatically detrended by its modeled relationship with April tmax. Vessel number was most highly correlated with the July tmax ( $r = -0.464$ ,  $p = 0.015$ , Supplementary Figure S2). Previous September VpdMax and March ppt were also highly correlated with the vessel number (Supplementary Figure S2). The vessel number was climatically detrended by its modeled relationship with the July tmax.

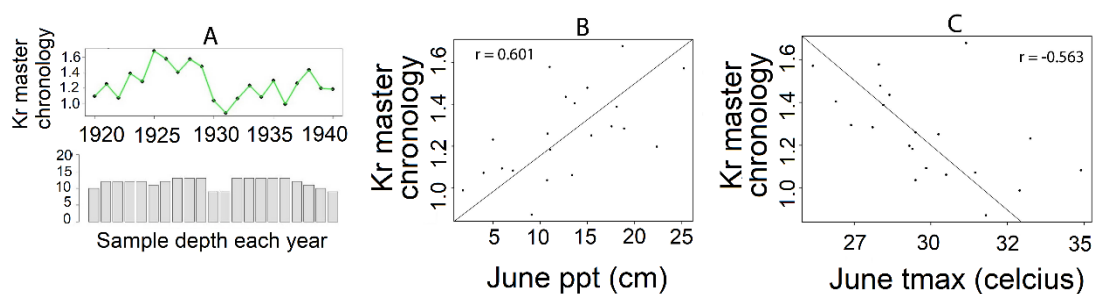


**Figure 4.** Selection of the climatic variable to detrend the age-detrended potential hydraulic conductivity (Kr) chronology (average of all the time-series, “Kr master chronology”), corresponding to the years 1920–1940, which had the highest sample depth for the period of 1895–1969. Abbreviations for climatic variables are as follows; ppt = sum precipitation in cm for each month, tmax = average maximum daily temperature for a given month in a year. June ppt had the highest magnitude of correlation with the Kr master chronology ( $r = 0.601$ ,  $p < 0.001$ ). The subsequent “age and climate” detrended time-series was detrended by the predicted relationship between each of the 14 time-series for Kr and June ppt.

Detrending by both age and climate led to moderate changes in results, compared to the effect of the first detrending by age. The variation in the MVA and Kr for lag0 and lag1 was reduced, resulting in significant differences with all other years ( $p < 0.001$ , Figure 3c). After climate-detrending, the vessel number was still not significantly different between lag0 and lag1 through to lag5 (Figure 3c). For all comparisons of MVA or Kr, lag1 was not significantly different from lag0. The significant declines in Kr during the lag0 and lag1 years were independent of the tree-related variables of age ( $r = -0.123$ ), the height of the cross-section above ground ( $r = 0.031$ ), and the percentage of circumference scarred ( $r = 0.192$ ) (Table 1). As Kr was not significantly correlated to the tree-related variables we did not proceed with model comparisons.

**Table 1.** Age, radius from pith (mm), and height about the bole from ground surface (m), along with percentage of the circumference scarred for each of the 14 trees used in this study.

Tree Number	Age	Radius from Pith When Scarred (mm)	Height of Section (m)	Percentage of Circumference Scarred
RUD01A	14	21.90	0.07	15
RUD01B	14	23.08	0.12	56
RUD05B	14	37.08	0.75	33
RUD11B	19	33.54	0.39	36
RUD13B	20	25.10	0.21	26
RUD28A	13	25.27	0.06	30
RUD36A	15	88.78	0.14	13
RUD39B	21	41.13	0.40	21
RUD40B	12	25.22	0.30	19
RUD25B	15	22.35	0.51	49
RUD36B	48	76.33	0.48	24
RUD13A	20	24.50	0.08	21
RUD41A	18	30.47	0.06	42
RUD35A	19	9.24	0.15	0.47

#### 4. Discussion

For this stand of white oak in northern Missouri, tree-ring specific potential hydraulic conductivity (i.e.,  $K_r$ ) was reduced significantly in the rings formed during and one year after fire injury. We are confident that this decline was a direct effect of fire injury as age- and climate-related trends were removed in calculating estimated hydraulic conductivity. After detrending for age and climate, we found MVA, not vessel number, was significantly reduced during the same time period post-fire, which explains the decline in  $K_r$ . In addition, we found no influence of percent circumference scarred, age when scarred, and size when scarred on the degree to which  $K_r$  (or MVA) temporarily declined after the fire in these trees. Here, we consider the physiological reasons leading to the significant temporary decline in MVA and  $K_r$  post-fire, how tree size and other factors may play a role and warrant further research, and discuss the implications of our work in the context of fire management and white oak drought susceptibility.

Both MVA and  $K_r$  were significantly reduced during the fire scar year and the year following. These reductions would not have been apparent without detrending for age and then climate. Negative exponential detrending of ring widths is essential in dendrochronology to remove the geometric effect of increasing stem area [44]. Likewise, MVA increased exponentially with age. This pattern is due to the requirement that vessels must maintain hydraulic efficiency as conduits lengthen and as trees increase in height and crowns expand with increasing amounts of foliage [36,45,46]. Climate-related effects also had to be removed; June ppt was the most highly correlated with  $K_r$  and April tmax with MVA. These climate correlations are consistent with studies done on oaks and other species from temperate regions [32–35,47,48] and correspond to current conditions when earlywood vessels differentiate from the vascular cambium. Furthermore, the previous winter climate had the second-strongest correlation with MVA, an effect seen in other studies with oak because it impacts earlywood vessel formation [49,50].

Physiologically, these correlations could be explained by water availability and hydraulic conditions near the time of vessel formation, which affects both the resources available for building lignified cell walls [51] and the production of lumens large enough to resist cavitation [52]. Interestingly, June is a period thought to be just beyond the most important period of earlywood vessel formation



in this region [53], and thus, it might be surprising that it is related to Kr. Compared to other studies focused on climate and effects on hydraulic properties in both temperate conifers and oaks, water availability during the summer, a time when the plant-water status is most vulnerable to drought, is commonly related to parameters associated with hydraulic conductivity [47,54]. In this study, summer climate, in general, was more related to vessel number than MVA; thus, there is a possibility that the manufacture of vessels may still proceed into the final weeks of spring depending on climatic conditions, which would affect potential hydraulic conductivity. In relatively drier temperate environments, years with wet late spring rains are related to increased proliferation of vessels in oaks [54–56]. Though these are sensible relationships, it should be cautioned that these climatic correlations occurred in a relatively short time, 1920–1940, an artifact of our method of selecting for trees with whole circumferences and the period with highest sample depth.

With the effects of age and climate variability minimized, fire injury had a negative effect on potential hydraulic conductivity for the scar year and the year immediately after. The clear negative effect of fire injury on MVA, compared to no discernable effect on vessel number, is the main effect on the resulting simultaneous decline in Kr. With tissue necrosis, it appears that white oaks retain the same number of vessels produced, perhaps at the expense of lumen area in the scar year and the year after. Decreased conductance in the year of the cambial injury may affect the manufacture of vessels in the following year, possibly due to a decline in carbon resources needed to build larger vessels [51]. Interestingly, the significant reduction in the potential hydraulic conductivity is not accompanied by reduced radial growth in these very same trees [6].

Stimulated growth evident in locally wider rings at the wound margins and in wound closure can compensate for wood volume not produced by the necrotic vascular cambium. However, that hyperplastic growth is anatomically distinct [26,57] including reduced vessel sizes. As previously described for conifers [58], stimulated wood production after fire injury reduces “notch stresses” that weaken stem structural integrity. Additionally, conifers shift their metabolism to produce traumatic resin canals that function in tree defense against pests and pathogens, which occurs at a physiological cost. That scenario was interpreted by [26] as an example of a tradeoff between growth and defense. In oak, the stimulated compensatory growth would reduce notch stresses while the decreased vessel size would likely increase wood strength and reduce the impact of pest and pathogen attack. The tradeoff in oak would, at least in part, be a reduced hydraulic efficiency. Considering the one year recovery time to return to pre-fire wound estimated conductivity, declines in conductance were relatively short-lived for these trees with a single fire scar. Declines in conductance from fire injury could be further amplified through repeated frequent fire-scarring or in years of drought that cause reduced growth [59,60].

A lack of effect of tree-related variables (e.g., age when scarred, size when scarred, and percent of circumference scarred) on the loss of potential hydraulic conductivity was surprising. Tree ages when scarred ranged from 12 to 48 years, although all but two were 20 years or younger. The same biased representation existed for scar size. [6] reported that scar size positively affected post-fire growth and time of wound closure in these same trees. Thus, we would expect age and/or tree size to at least have some buffering influence on loss of potential hydraulic conductivity, given increased thickness of bark [61], as well as the fact that closely related oak species see an inverse relationship between age/size and percent of the circumference scarred [14]. However, our sample of age and tree size was likely not adequate enough for this relationship to be expressed. Furthermore, for our 14 trees, age was not related to percent of circumference scarred, and tree size was only weakly correlated to age.

Similar future studies will need to be cognizant of capturing a better representation of tree age and size to investigate these relationships with the degree of scarring further, as well as a greater sampling of conditions which lead to different degrees of scarring, such as fire intensity, topographic position, and heat exposure time. Variable fire timing could also be important and should be considered since the season of fires in relation to the timing of tree growth could differentially affect Kr, especially for oaks with large early wood vessels.

## 5. Conclusions

Potential hydraulic conductivity in white oak was reduced for the year of and the first year after fire injury. Since wounds may take several years to close depending on the percent of circumference scarred [6], overall tree vitality must be further considered for areas which may receive frequent fires or other disturbances that result in cambial injury. Furthermore, drought during recovery from injury may act synergistically with reduced hydraulic conductivity to negatively affect stocking rates and the overall wood quality. Further research on white oak and other dominant trees would benefit identification how the loss of potential hydraulic conductivity may be a function of age, size, and proportion of the stem circumference scarred from fire or other factors. With this information, we may be better able to predict the impact of various management options, especially in years where the hydraulic function may already be under stress due to drought.

**Supplementary Materials:** The following are available online at <http://www.mdpi.com/1999-4907/10/9/812/s1>. Figure S1: Three paneled-figure showing change in Kr, MVA, and vessel number as a function of age in both a linear (left) and exponential (right) fit. Fitting an exponential curve on this relationship explained more variance for Kr and MVA, while a linear fit explained slightly more variance for vessel number. The above curves were used to determine which type of age detrending was to be applied to the raw values of Kh, MVA, and number of vessels for the 11 year time-series for each disc. Figure S2: Three paneled-figure showing heatmaps and associated tables for monthly climate correlation coefficients and their associated p values (derived from bootstrapping, only the top 15 correlations) for potential hydraulic conductivity Kr (top), mean vessel area MVA, and vessel number (bottom). Max Temp (tmax), precipitation sum for each month in cm (ppt), and maximum daily vapor pressure average for each month (VpdMax) for each month within the 24 month period were correlated with the age-detrended “transect” values for Kr, MVA, and vessel number. Heatmaps only show through the current Sep, since we did not consider the correlations after this monthly period, though these correlation coefficients may still be found in the accompanying table if the relationship is one of the top 15 correlations.

**Author Contributions:** Author contributions are as follows: conceptualization—J.R.D., M.C.S. and K.T.S.; methodology—J.R.D., M.C.S. and K.T.S.; software—J.R.D.; validation—J.R.D.; formal analysis—J.R.D.; investigation—J.R.D. and M.C.S.; resources—J.R.D. and M.C.S.; data curation—J.R.D. and M.C.S.; writing—original draft preparation—J.R.D.; writing—review and editing—J.R.D., M.C.S., K.T.S., and D.C.D.; visualization—J.R.D., M.C.S. and K.T.S.; supervision—M.C.S.; project administration—M.C.S., K.T.S., and D.C.D.; funding acquisition—K.T.S. and D.C.D.

**Funding:** Funding for this research was provided by the U.S. Forest Service, Northern Research Station. The Missouri Department of Conservation provided access to fire-scarred trees and permission for sampling. Field and laboratory assistance was provided by Adam Zimmerman and Erin Abadir.

**Acknowledgments:** The authors would like to thank Adam Zimmerman and Erin Abadir for field and laboratory assistance.

**Conflicts of Interest:** The authors declare no conflict of interest.

## References

1. Mooney, H.A.; Dunn, E.L. Convergent evolution of Mediterranean-climate evergreen sclerophyll shrubs. *Evolution* **1970**, *24*, 292–303. [[CrossRef](#)] [[PubMed](#)]
2. Watts, W.A. Late Quaternary vegetation of central Appalachia and the New Jersey coastal plain. *Ecol. Monogr.* **1979**, *49*, 427–469. [[CrossRef](#)]
3. Zavala, M.A.; Espelta, J.M.; Retana, J. Constraints and trade-offs in Mediterranean plant communities: The case of holm oak-Aleppo pine forests. *Bot. Rev.* **2000**, *66*, 119–149. [[CrossRef](#)]
4. Umbanhowar, C.E.; Camill, P.; Geiss, C.E.; Teed, R. Asymmetric vegetation responses to mid-Holocene aridity at the prairie–forest ecotone in south-central Minnesota. *Quat. Res.* **2006**, *66*, 53–66. [[CrossRef](#)]
5. Smith, K.T.; Sutherland, E.K. Fire-scar formation and compartmentalization in oak. *Can. J. For. Res.* **1999**, *29*, 166–171. [[CrossRef](#)]
6. Stambaugh, M.C.; Smith, K.T.; Dey, D.C. Fire scar growth and closure rates in white oak (*Quercus alba*) and the implications for prescribed burning. *For. Ecol. Manag.* **2017**, *391*, 396–403. [[CrossRef](#)]
7. Abrams, M.D. Fire and the development of oak forests. *BioScience* **1992**, *42*, 346–353. [[CrossRef](#)]
8. Albrecht, M.A.; McCarthy, B.C. Effects of prescribed fire and thinning on tree recruitment patterns in central hardwood forests. *For. Ecol. Manag.* **2006**, *226*, 88–103. [[CrossRef](#)]

9. Hutchinson, T.F.; Long, R.P.; Rebbeck, J.; Sutherland, E.K.; Yaussy, D.A. Repeated prescribed fires alter gap-phase regeneration in mixed-oak forests. *Can. J. For. Res.* **2012**, *42*, 303–314. [[CrossRef](#)]
10. Nowacki, G.J.; Abrams, M.D. The demise of fire and “mesophication” of forests in the eastern United States. *AIBS Bull.* **2008**, *58*, 123–138. [[CrossRef](#)]
11. Arthur, M.A.; Alexander, H.; Dey, D.C.; Schweitzer, C.J.; Loftis, D.L. Refining the oak-fire hypothesis for management of oak-dominated forests of the eastern United States. *J. For.* **2012**, *110*, 257–266. [[CrossRef](#)]
12. Guyette, R.P.; Muzika, R.M.; Dey, D.C. Dynamics of an anthropogenic fire regime. *Ecosystems* **2002**, *5*, 472–486.
13. McEwan, R.W.; Hutchinson, T.F.; Long, R.P.; Ford, R.D.; McCarthy, B.C. Temporal and spatial patterns of fire occurrence during the establishment of mixed-oak forests in eastern North America. *J. Veg. Sci.* **2007**, *18*, 655–664. [[CrossRef](#)]
14. Stambaugh, M.C.; Guyette, R.P. Fire regime of an Ozark wilderness area, Arkansas. *Am. Midl. Nat.* **2006**, *156*, 237–251. [[CrossRef](#)]
15. Stambaugh, M.C.; Marschall, J.M.; Abadir, E.R.; Jones, B.C.; Brose, P.H.; Dey, D.C.; Guyette, R.P. Wave of fire: An anthropogenic signal in historical fire regimes across central Pennsylvania, USA. *Ecosphere* **2018**, *9*, 1–28. [[CrossRef](#)]
16. Devivo, M.S. Indian use of fire and land clearance in the Southern Appalachians. In *Fire and the Environment: Ecological and Cultural Perspectives*; General Technical Report SE-09; US Department of Agriculture, Forest Service: Washington, DC, USA, 1991; pp. 306–309.
17. Williams, G.W. References on the American Indian Use of Fire in Ecosystems. 1994. Available online: <http://wings.buffalo.edu/anthropology/Documents/firebib.txt> (accessed on 24 January 2019).
18. Dey, D.C.; Schweitzer, C.J. Timing fire to minimize damage in managing oak ecosystems. In *Proceedings of the 17th Biennial Southern Silvicultural Research Conference*; Shreveport, L.A., Gordon, H.A., Connor, K.F., Haywood, J.D., Eds.; USDA Forest Service, Southern Research Station: Asheville, NC, USA, 2015; p. 11.
19. Ryan, K.C.; Knapp, E.E.; Varner, J.M. Prescribed fire in North American forests and woodlands: History, current practice, and challenges. *Front. Ecol. Environ.* **2013**, *11*, 15–24. [[CrossRef](#)]
20. *An Assessment of Missouri Forest Health Issues and Their Impact on Future Management Priorities*; Missouri Forest Products Association (MFPA): Jefferson City, MO, USA, 2013; p. 24.
21. Loomis, R.M. *Predicting the Losses in Sawtimber Volume and Quality from Fire in Oak-Hickory Forests*; Res. Pap. NC-104; U.S. Department of Agriculture, Forest Service, North Central Forest Experiment Station: St. Paul, MN, USA, 1975; p. 6.
22. Guyette, R.P.; Stambaugh, M.C.; Stevenson, A.; Muzika, R. *Prescribed Fire Effects on the Wood Quality of Oak (Quercus species) and Shortleaf Pine (Pinus echinata)*; Final Report Prepared for the Missouri; Department of Conservation: Jefferson City, MO, USA, 2008; p. 115.
23. Marschall, J.M.; Guyette, R.P.; Stambaugh, M.C.; Stevenson, A.P. Fire damage effects on red oak timber product value. *For. Ecol. Manag.* **2014**, *320*, 182–189. [[CrossRef](#)]
24. Wiedenbeck, J.; Smith, K.T. Hardwood management, tree wound response, and wood product value. *For. Chron.* **2018**, *94*, 292–306.
25. Smith, K.T.; Sutherland, E.K. Resistance of eastern hardwood stems to fire injury and damage. In *Fire in Eastern Oak Forests: Delivering Science to Land Managers, Proceedings of a Conference, Columbus, OH, USA, 15–17 November 2005*; General Technical Report NRS-P-1; Dickinson, M.B., Ed.; U.S. Department of Agriculture, Forest Service, Northern Research Station: Newtown Square, PA, USA, 2006; pp. 210–217.
26. Smith, K.T. Compartmentalization, resource allocation, and wood quality. *Curr. For. Rep.* **2015**, *1*, 8–15. [[CrossRef](#)]
27. Pearce, R.B. Antimicrobial defenses in the wood of living trees. *New Phytol.* **1996**, *132*, 203–233. [[CrossRef](#)]
28. Tyree, M.T.; Zimmermann, M.H. *Xylem Structure and the Ascent of Sap*; Springer: Berlin/Heidelberg, Germany, 2002; p. 283.
29. Cochard, H.; Tyree, M.T. Xylem dysfunction in Quercus: Vessel sizes, tyloses, cavitation and seasonal changes in embolism. *Tree Physiol.* **1990**, *6*, 393–407. [[CrossRef](#)] [[PubMed](#)]
30. Michaletz, S.T.; Johnson, E.A.; Tyree, M.T. Moving beyond the cambium necrosis hypothesis of post-fire tree mortality: Cavitation and deformation of xylem in forest fires. *New Phytol.* **2012**, *164*, 254–263. [[CrossRef](#)] [[PubMed](#)]
31. Michaletz, S.T. Xylem dysfunction in fires: Towards a hydraulic theory of plant responses to multiple disturbance stressors. *New Phytol.* **2018**, *217*, 1391–1393. [[CrossRef](#)] [[PubMed](#)]

32. González-González, B.D.; Rozas, V.; García-González, I. Earlywood vessels of the sub-Mediterranean oak *Quercus pyrenaica* have greater plasticity and sensitivity than those of the temperate *Q. petraea* at the Atlantic–Mediterranean boundary. *Trees* **2014**, *28*, 237–252. [[CrossRef](#)]
33. Carrer, M.; von Arx, G.; Castagneri, D.; Petit, G. Distilling allometric and environmental information from time series of conduit size: The standardization issue and its relationship to tree hydraulic architecture. *Tree Physiol.* **2015**, *35*, 27–33. [[CrossRef](#)] [[PubMed](#)]
34. Castagneri, D.; Petit, G.; Carrer, M. Divergent climate response on hydraulic-related xylem anatomical traits of *Picea abies* along a 900-m altitudinal gradient. *Tree Physiol.* **2015**, *35*, 1378–1387. [[CrossRef](#)] [[PubMed](#)]
35. Wilkinson, S.; Ogée, J.; Domec, J.-C.; Rayment, M. Wingate. Biophysical modelling of intra-ring variations in tracheid features and wood density of *Pinus pinaster* trees exposed to seasonal droughts. *Tree Physiol.* **2015**, *35*, 305–318. [[CrossRef](#)] [[PubMed](#)]
36. Daly, C.; Gibson, W.P.; Doggett, M.; Smith, J.; Taylor, G. Up-to-Date Monthly Climate Maps for the Conterminous United States. In Proceedings of the 14th American Meteorological Society Conference on Applied Climatology, Seattle, WA, USA, 13–16 January 2004.
37. Stokes, M.; Smiley, T. *Introduction to Tree-Ring Dating*; Univ. of Chicago Press: Chicago, IL, USA, 1968; p. 73.
38. Holmes, R.L. Computer-assisted quality control in tree-ring dating and measurements. *Tree Ring Bull.* **1983**, *43*, 69–78.
39. Grissino-Mayer, H.D. Evaluating crossdating accuracy: A manual and tutorial for the computer program COFECHA. *Tree Ring Res.* **2001**, *57*, 205–221.
40. Von Arx, G.; Carrer, M. ROXAS—A new tool to build centuries-long tracheid-lumen chronologies in conifers. *Dendrochronologia* **2014**, *32*, 290–293. [[CrossRef](#)]
41. Lewis, A.M.; Boose, E.R. Estimating Volume Flow Rates Through Conduits. *Am. J. Bot.* **1995**, *82*, 1111–1116. [[CrossRef](#)]
42. Warnes, G.R.; Bolker, B.; Bonebakker, L.; Gentleman, R.; Huber, W.; Liaw, A.; Lumley, T.; Maechler, M.; Magnusson, A.; Moeller, S.; et al. gplots: Various R programming tools for plotting data. *R Package Version* **2009**, *2*, 1.
43. RStudio Team. *RStudio: Integrated Development for R*; RStudio, Inc.: Boston, MA, USA, 2017; Available online: <http://www.rstudio.com> (accessed on 3 February 2019).
44. Cook, E.R.; Holmes, R.L. Guide for Computer Program ARSTAN. *Int. Tree-Ring Data Bank Program Libr. Version* **1996**, *2*, 75–87.
45. West, G.B.; Brown, J.H.; Enquist, B.J. A general model for the structure and allometry of plant vascular systems. *Nature* **1999**, *400*, 664–667. [[CrossRef](#)]
46. Anfodillo, T.; Carraro, V.; Carrer, M.; Fior, C.; Rossi, S. Convergent tapering of xylem conduits in different woody species. *New Phytol.* **2006**, *169*, 279–290. [[CrossRef](#)]
47. Bryukhanova, M.; Fonti, P. Xylem plasticity allows rapid hydraulic adjustment to annual climatic variability. *Trees* **2013**, *27*, 485–496. [[CrossRef](#)]
48. Xu, J.; Lu, J.; Bao, F.; Evans, R.; Downes, G.M. Climate response of cell characteristics in tree rings of *Picea crassifolia*. *Holzforschung* **2013**, *67*, 217–225. [[CrossRef](#)]
49. García-González, I.; Eckstein, D. Climatic signal of earlywood vessels of oak on a maritime site. *Tree Physiol.* **2003**, *23*, 497–504. [[CrossRef](#)]
50. Fonti, P.; García-González, I. Earlywood vessel size of oak as potential proxy for spring precipitation in mesic sites. *J. Biogeogr.* **2008**, *35*, 2249–2257. [[CrossRef](#)]
51. Plomion, C.; Leprovost, G.; Stokes, A. Wood formation in trees. *Plant Physiol.* **2001**, *127*, 1513–1523. [[CrossRef](#)]
52. Tyree, M.T.; Sperry, J.S. Vulnerability of xylem to cavitation and embolism. *Annu. Rev. Plant Biol.* **1989**, *40*, 19–36. [[CrossRef](#)]
53. Voelker, S.L.; Noirot-Cosson, P.E.; Stambaugh, M.C.; McMurry, E.R.; Meinzer, F.C.; Lachenbruch, B.; Guyette, R.P. Spring temperature responses of oaks are synchronous with North Atlantic conditions during the last deglaciation. *Ecol. Monogr.* **2012**, *82*, 169–187. [[CrossRef](#)]
54. Eilmann, B.; Zweifel, R.; Buchmann, N.; Fonti, P.; Rigling, A. Drought induced adaptation of xylem in Scots pine and pubescent oak. *Tree Physiol.* **2009**, *29*, 1011–1020. [[CrossRef](#)] [[PubMed](#)]
55. Woodcock, D.W. Climate sensitivity of wood-anatomical features in a ring-porous oak (*Quercus macrocarpa*). *Can. J. For. Res.* **1989**, *19*, 639–644. [[CrossRef](#)]

56. Tardif, J.C.; Conciatori, F. Influence of climate on tree rings and vessel features in red oak and white oak growing near their northern distribution limit, southwestern Quebec, Canada. *Can. J. For. Res.* **2006**, *36*, 2317–2330. [[CrossRef](#)]
57. Fink, S. *Pathological and Regenerative Plant Anatomy*; Gebruder Borntraeger: Stuttgart, Germany, 1999; p. 1095.
58. Smith, K.T.; Arbellay, E.; Falk, D.A.; Sutherland, E.K. Macroanatomy and compartmentalization of recent fire scars in three North American conifers. *Can. J. For. Res.* **2016**, *46*, 535–542. [[CrossRef](#)]
59. Kabrick, J.M.; Dey, D.C.; Jensen, R.G.; Wallendorf, M. The role of environmental factors in oak decline and mortality in the Ozark Highlands. *For. Ecol. Manag.* **2008**, *255*, 1409–1417. [[CrossRef](#)]
60. Fan, Z.; Fan, X.; Crosby, M.K.; Moser, W.K.; He, H.; Spetich, M.A.; Shifley, S.R. Spatio-temporal trends of oak decline and mortality under periodic regional drought in the Ozark Highlands of Arkansas and Missouri. *Forests* **2012**, *3*, 614–631. [[CrossRef](#)]
61. Howard, E.T. Bark structure of southern upland oaks. *Wood Fiber Sci.* **2007**, *9*, 172–183.



© 2019 by the authors. Licensee MDPI, Basel, Switzerland. This article is an open access article distributed under the terms and conditions of the Creative Commons Attribution (CC BY) license (<http://creativecommons.org/licenses/by/4.0/>).